JACS
JOURNAL OF THE AMERICAN CHEMICAL SOCIETY
Article
pubs.acs.org/JACS

In Vitro and Cellular Self-Assembly of a Zn-Binding Protein Cryptand via Templated Disulfide Bonds

Annette Medina-Morales, Alfredo Perez, Jeffrey D. Brodin, and F. Akif Tezcan*

Department of Chemistry and Biochemistry, University of California, San Diego, La Jolla, California 92093-0356, United States

Supporting Information

ABSTRACT: Simultaneously strong and reversible through redox chemistry, disulfide bonds play a unique and often irreplaceable role in the formation of biological and synthetic assemblies. In an approach inspired by supramolecular chemistry, we report here that engineered noncovalent interactions on the surface of a monomeric protein can template its assembly into a unique cryptand-like protein complex ($^{C81/C96}$RIDC1$_4$) by guiding the selective formation of multiple disulfide bonds across different interfaces. Owing to its highly interconnected framework, $^{C81/C96}$RIDC1$_4$ is well preorganized for metal coordination in its interior, can support a large internal cavity surrounding the metal sites, and can withstand significant alterations in inner-sphere metal coordination. $^{C81/C96}$RIDC1$_4$ self-assembles with high fidelity and yield in the periplasmic space of *E. coli* cells, where it can successfully compete for Zn(II) binding.

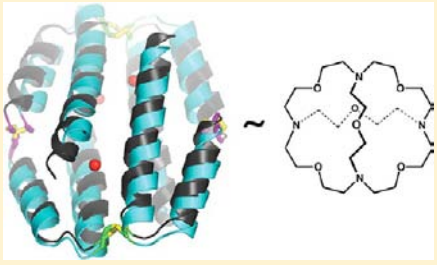

INTRODUCTION

Chemical templating, generally defined as the use of noncovalent interactions to spatially organize molecules to promote the selective formation of covalent bonds between them,[1,2] is pervasive in nature. While the polymerization of DNA is the first example that comes to mind, essentially all enzyme-catalyzed bond-forming reactions can be considered as being templated by the noncovalent framework of enzymes. Templating has also been a powerful strategy in the synthesis of complex, covalently linked architectures.[3,4] In coordination chemistry, metal ions have long been exploited to direct the formation of macrocyclic scaffolds,[5,6] ranging from phthalocyanines as initial examples[7] to more complex polycyclic compounds that serve as selective hosts for metal ions.[8,9] Likewise, in supramolecular chemistry, templating has enabled the synthesis of a diverse array of challenging synthetic targets, including interlocked structures such as rotaxanes, catenanes, and molecular knots.[10−13] The scope of such synthetic efforts in chemical templating has been expanded through the use of biological building blocks such as DNA,[14] the development of self-replicating peptides,[15−17] covalent capture strategies,[18−20] and, broadly, the advent of dynamic combinatorial/covalent chemistry.[21−23] These advances in synthetic templating strategies prompted us to explore whether they can also be employed toward the construction of discrete multiprotein assemblies, which execute most of the fundamental cellular tasks and, thus, are primarily responsible for biological complexity. Specifically, we asked if self-complementary, noncovalent interactions built onto a certain facet of a protein building block could yield a stable, supramolecular architecture by directing the selective formation of multiple disulfide bonds on other facets.

Quaternary protein structures and supramolecular protein architectures are assembled primarily through extensive noncovalent interactions, which form multiple interfaces between the constituent building blocks. The bottom-up construction of protein assemblies solely through the design and engineering of such noncovalent interfaces is a significant challenge, as, by necessity, each of these interfaces has to be extensive. Nevertheless, efforts in this area have started to yield impressive architectures, such as 2D layers[24] and cagelike architectures,[25−27] particularly by exploiting supramolecular symmetry as a primary design element,[28] which leads to cooperativity between the interfaces.

In this regard, disulfide bonds are particularly attractive as structure building tools, as they are considerably stronger (bond dissociation energy ≈ 60 kcal/mol)[29] than noncovalent interactions and thus would not require the design or engineering of extensive molecular surfaces. Indeed, disulfide bond engineering is a well-established strategy to stabilize existing (i.e., already evolved) protein folds[30,31] or protein−protein interfaces[32−35] and to covalently link protein building blocks for spatial preorganization[27] or symmetrization[36] with minimal structural perturbation. In addition, disulfide bonds are reversible through two-electron reduction and responsive to external stimuli, such as pH and ionic strength.[37] This unique combination of stability, reversibility, and stimuli-responsiveness accounts for not only the prevalence of disulfide bonds in biological systems but also their increasing use in synthetic supramolecular chemistry.[21−23] Despite these advantages and some notable successes in peptide self-assembly,[38] disulfide bonds are not commonly—if at all—exploited *in multiples* for

Received: May 27, 2013
Published: August 1, 2013

   dx.doi.org/10.1021/ja405318d | *J. Am. Chem. Soc.* 2013, 135, 12013−12022

the bottom-up assembly of discrete/closed supramolecular protein architectures. There are several reasons. First, this goal would necessitate the formation of several disulfide bonds in a selective fashion during protein self-assembly. This, in turn, would require the programming of a structural bias for positioning (i.e., templating) the correct cysteine pairs across from one another, a grand challenge on its own.[39] Second, this goal would necessitate the consideration of the multiple assembly pathways involving alternative cysteine pairs, which may form deep kinetic traps.[40] Third, protein constructs with multiple thiol groups are difficult to produce and handle in experimental settings.[41] To our knowledge, there are no designed protein architectures that self-assemble via the formation of multiple disulfide bonds across different interfaces.

Recently, we have applied design strategies of supramolecular coordination chemistry to control the assembly of monomeric proteins into closed or infinite protein superstructures.[42−44] Our approach is based on the premise that the strength and directionality of metal coordination interactions built onto protein surfaces can direct the assembly of symmetrical protein superstructures, whose interfaces can be subsequently stabilized through the introduction of favorable noncovalent interactions around the metal nuclei. Here, we show that such engineered noncovalent interactions can template the selective formation of multiple disulfide bonds to yield a novel, macrocyclic superprotein architecture, whose assembly is uncoupled from metal coordination. This assembly, $^{C81/C96}$RIDC1$_4$, features four interconnected disulfide bonds in a cryptand-like topology. By virtue of its topology and due to the fact that its self-assembly no longer depends on metal binding, $^{C81/C96}$RIDC1$_4$ is highly preorganized for metal coordination, has a large internal cavity surrounding the metal sites, and is resistant to alterations in inner-sphere metal coordination, all of which constitute challenging targets for protein design. What is more, $^{C81/C96}$RIDC1$_4$ correctly self-assembles and incorporates Zn(II) ions in bacterial cells, thus forging a link between synthetic supramolecular chemistry and synthetic biology.

RESULTS AND DISCUSSION

Design of $^{C81/C96}$RIDC1. The protein construct $^{C81/C96}$RIDC1 (the C81/C96 double mutant of Rosetta Interface Designed Cytochrome 1, Figure 1a), which is the monomeric building block for the $^{C81/C96}$RIDC1$_4$ tetramer, is a derivative of the four-helix-bundle hemeprotein, cytochrome cb_{562}.[45] We previously reported a first-generation cytochrome cb_{562} mutant (MBPC1; Metal Binding Protomer of Cytochrome 1), which was engineered on its surface with metal coordinating residues (orange sticks in Figure 1a and b).[46] Upon binding various divalent transition metal ions, MBPC1 was observed to assemble into discrete assemblies whose compositions and supramolecular symmetries were dictated by the stereochemical preferences of the metal ions.[47] In particular, tetrahedral coordination of Zn(II) by residues His63, Asp74, His73, and His77 led to the formation of a tetrameric, D_2 symmetric assembly (Figure 1b).[46] Owing to its dihedral symmetry, Zn$_4$:MBPC1$_4$ possesses an interlocked architecture with particularly extensive (~5000 Å^2 total) but nonfavorable interfacial interactions, which are distributed over three pairs of orthogonal, C_2-symmetric interfaces (*i1*, *i2*, and *i3*) (Figure 1b). These three interfaces are interconnected but nonoverlapping. Consequently, the stabilization of any of these interfaces should also favor the formation of the other two

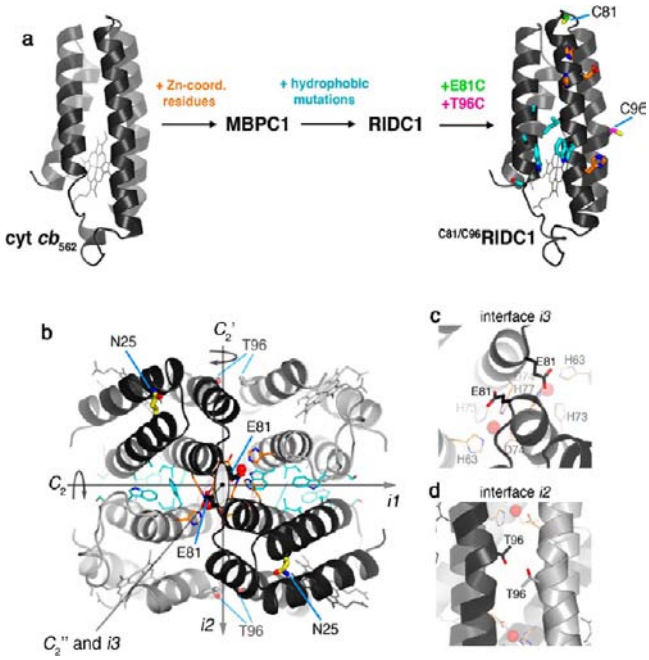

Figure 1. Structural features of cyt cb_{562} central to the design of $^{C81/C96}$RIDC1. (a) Three stages of mutations made on cyt cb_{562} to convert it to $^{C81/C96}$RIDC1. The mutated residues to construct MBPC1 and RIDC1 are shown as orange and cyan-colored sticks, respectively. Two engineered surface cysteines, C81 and C96, are highlighted in green and magenta, respectively. (b) *D2* symmetric structure of Zn$_4$:RIDC1$_4$ viewed down the C_2'' axis, along which interface *i3* is formed. *i1* and *i2* are formed along the orthogonal C_2 and C_2' axes, which lie parallel to the plane of view. Hydrophobic residues inserted into *i1*, as well as the symmetrically related pairs of Glu81 and Thr96 residues in *i2* and *i3*, which are mutated to Cys, are highlighted. (c, d) Close-up views of Glu81 and Thr96.

interfaces (as well as the entire assembly), yet, from a protein engineering perspective, they should be independently addressable for redesign.

We had shown that *i1*, the most extensive and close-packed of the three interfaces, can be stabilized through the incorporation of six mostly hydrophobic mutations (cyan sticks in Figure 1a and b) onto the MBPC1 monomer surface to generate RIDC1 and subsequently its Zn-mediated tetramer Zn$_4$:RIDC1$_4$, which is isostructural with Zn$_4$:MBPC1$_4$.[48] Indeed, in the absence of Zn(II) binding, RIDC1 was able to dimerize ($K_{d,dimer}$ = 26 μM) via the engineered hydrophobic interactions in an antiparallel fashion, as was observed in the Zn-driven tetrameric architecture.[48] *i3* is too small for stabilization through noncovalent interactions, and though extensive, *i2* features too wide a clearance between monomers for efficient hydrophobic packing. Nevertheless, both *i2* and *i3* present two pairs of symmetrically related residue positions (96−96′ in *i2* and 81−81′ in *i3*) across from one another in close proximity for potentially forming Cys−Cys disulfide bonds (C_α−C_α distances <5.6 Å) (Figure 1c and d). Indeed, 96−96′ disulfide bonds were shown to be readily accommodated in the Zn$_4$:RIDC1$_4$ tetramer.[49] From a self-assembly viewpoint, it is important to note that, with only one surface Cys present, selectivity is not an issue, as the desired disulfide bond will always form. This is not the case when two Cys residues are present on the same protein building block, which may lead to the formation of a mixture of disulfide bonds and thereby to heterogeneous aggregates. Here, we set out to take

dx.doi.org/10.1021/ja405318d | J. Am. Chem. Soc. 2013, 135, 12013−12022

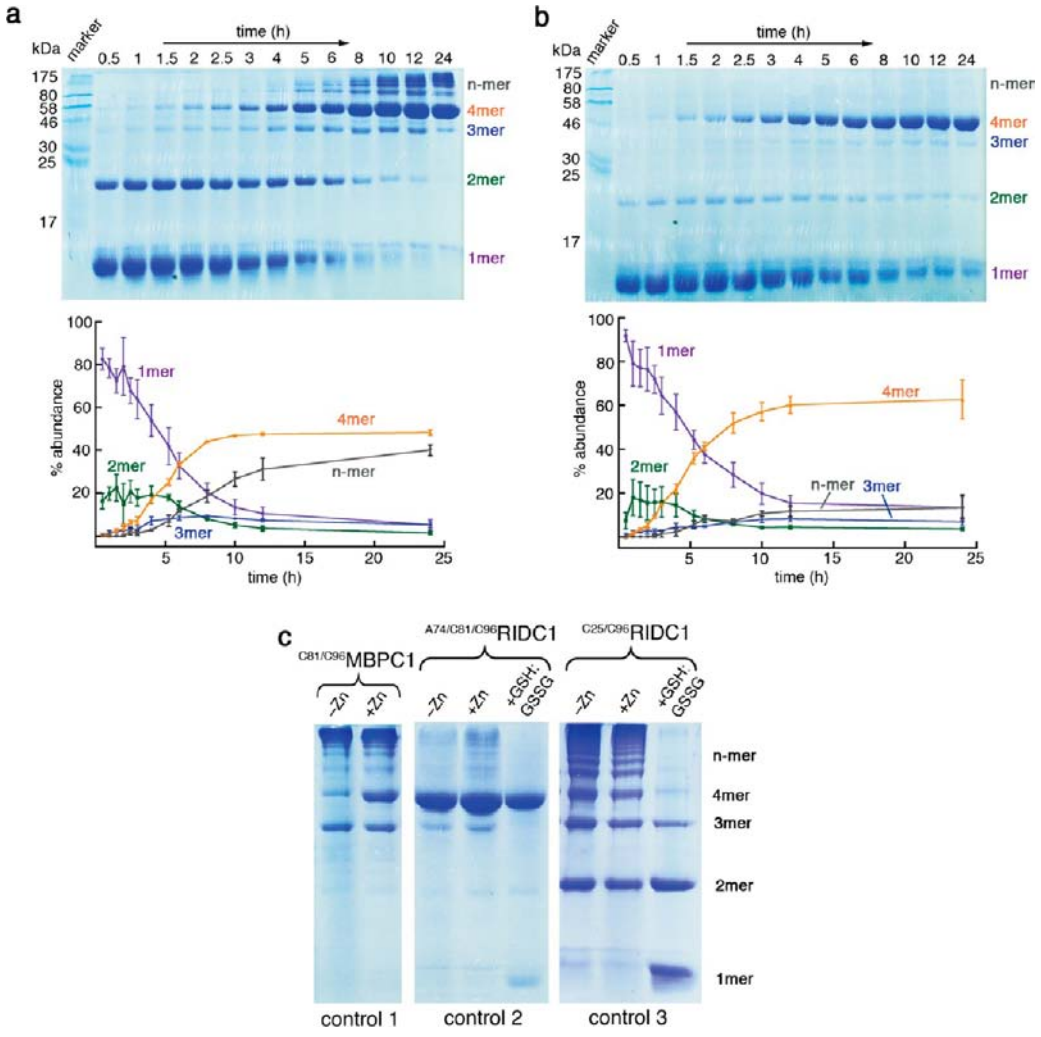

Figure 2. *In vitro* disulfide-mediated self-assembly of $^{C81/C96}$RIDC1 at room temperature. (a) Time-course of the oxidative self-assembly of $^{C81/C96}$RIDC1 (50 μM) at pH 7 as characterized by SDS-PAGE under nonreducing conditions. (b) Time-course of the disulfide-mediated self-assembly of $^{C81/C96}$RIDC1 (50 μM) at pH 7 in the presence of 950 μM GSH and 50 μM GSSG. In parts a and b, the upper panels represent the images of the actual gels, and the bottom panels show the relative integrated intensities of the observed bands in the gels. The data are the mean of three measurements ± 1 SD. (c) Disulfide-mediated self-assembly of the three control variants, $^{C81/C96}$MBPC1, $^{A74/C81/C96}$RIDC1, and $^{C25/C96}$RIDC1, in the presence or absence of Zn or GSH/GSSG redox buffer, as monitored by SDS-PAGE electrophoresis under nonreducing conditions.

advantage of the symmetry of the Zn-templated tetramer and probe whether complementary, noncovalent interactions built into the *i1* interfaces can template the correct formation of four disulfide bonds (2 × Cys96-Cys96′ and 2 × Cys81-Cys81′) across the other two interfaces during self-assembly. We thus prepared the $^{C81/C96}$RIDC1 mutant through Glu81Cys and Thr96Cys mutations (Figure 1a).

Oxidative Self-Assembly of $^{C81/C96}$RIDC1. In the first set of experiments, solutions of isolated $^{C81/C96}$RIDC1 (typically 50 μM in concentration) were subjected to air oxidation at room temperature, and the time-course for the formation of disulfide-containing products was determined by gel electrophoresis (SDS-PAGE) under denaturing and nonreducing conditions. The major products were a distinct tetrameric species (48 ± 2% in abundance) and various higher order aggregates (40 ± 3%) (Figure 2a, top panel). These products formed over the course of 24 h following a noticeable induction phase, during which a dimeric intermediate was transiently populated (Figure 2a, bottom panel). A small, but persistent population (5−8%) of trimeric species was also detected. At 35 °C, the rates of monomer consumption and tetramer/polymer production were considerably higher, and the induction period was largely eliminated, although the product distribution did not change significantly (Figure S1 of the Supporting Information (SI)). Inclusion of equimolar Zn(II) in the reaction mixture altered neither the rate of formation significantly nor the distribution of products (Figure S2 of the SI), suggesting that Zn(II) coordination does not contribute to the stability of the self-assembly intermediates.

These initial results can be explained in terms of the proposed self-assembly model shown in Figure 3. According to this model, the predominant pathway proceeds through the reversible dimerization of $^{C81/C96}$RIDC1 (species 1) through the complementary interactions in *i1* that yield a dimer (species 2). This proposed dimer has all four Cys residues correctly oriented for the formation of the closed tetramer (species 5), which is supported by the previously observed antiparallel arrangement of the metal-independent $RIDC1_2$ dimer.[48] The remaining fraction of monomers can form disulfide-linked dimers (detectable as such in SDS-PAGE) that are either correctly paired (species 3) to form the closed tetramer through complementary *i1* interactions or incorrectly paired

dx.doi.org/10.1021/ja405318d | J. Am. Chem. Soc. 2013, 135, 12013−12022

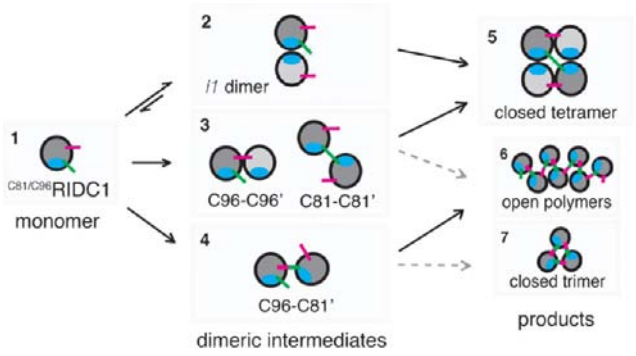

Figure 3. Proposed scheme for the disulfide-mediated self-assembly of $^{C81/C96}$RIDC1. The dark- or light-gray-shaded circles correspond to the views of the four-helix protein building blocks from top or bottom as shown in Figure 1b. Dotted arrows indicate alternative pathways of oligomer formation. Residues C81 and C96 are illustrated as green and magenta sticks, and the hydrophobic residues in *i1* as cyan patches, matching the coloring scheme in Figure 1.

(species 4), which would lead higher order aggregates (species 6) or a closed trimer (species 7).

Given that disulfide bond formation is largely irreversible under these experimental conditions, the templated formation of the closed $^{C81/C96}$RIDC1$_4$ tetramer should be under kinetic control, whereby the noncovalent *i1* interactions geometrically favor the formation of the four, correct disulfide bonds. Under the assumption that the closed tetramer—which has all of its interfaces correctly formed—is also the thermodynamically most favored product among those shown in Figure 3, we surmised that its formation should be favored under conditions that promote reversible disulfide bond formation (i.e., where all steps in Figure 3 operate under equilibrium). Toward this end, we utilized a redox buffer system containing reduced and oxidized forms of glutathione (GSH and GSSG, respectively). At a molar ratio of 19:1 GSH/GSSG (combined concentration of 1 mM, E'_{pH7} = −187 mV),[50] the yield for the tetramer after 1 day of oxidation indeed rose from 48% to 63 ± 9% (Figure 2b). As expected from a system under thermodynamic control, this increase in the yield compared to the non-redox-buffered system came primarily at the expense of the less stable, polymeric species, whose abundance decreased from 40% to 13 ± 6%. Under more oxidizing conditions (1:19 GSH/GSSG at 1 mM total concentration, E'_{pH7} = −77 mV),[50] the product distribution did not change significantly, although the reaction proceeded more rapidly, as expected (Figure S3 of the SI). Treatment with the strong reducing agent dithiothreitol (DTT, E'_{pH7} = −330 mV)[51] led to complete dissociation of all oligomeric products. Our results thus indicate that the disulfide bonds in $^{C81/C96}$RIDC1$_4$ have reduction potentials (−200 to −300 mV) typical of natural systems and that even small amounts of GSH are sufficient to catalyze reversible disulfide exchange and ensure thermodynamic control.

To further probe the validity of our model, we prepared three control variants and examined their self-assembly under oxidative conditions. The first variant, $^{C81/C96}$MBPC1, had the same two Cys residues but lacked the hydrophobic surface residues that stabilize and preorient the *i1* interface. In contrast to $^{C81/C96}$RIDC1, $^{C81/C96}$MBPC1 did not display any preference for tetramer formation: after ∼16 h of air oxidation, the main products were higher-order aggregates (∼80% in abundance) with only ∼7% in tetrameric form (Figure 2c, left panel). In this case, however, the addition of equimolar Zn(II) did yield a noticeable increase in the tetramer population (∼20%), suggesting that Zn(II) coordination may help template the formation of the closed tetramer in the absence of the directing *i1* interactions.

To conclusively establish that the templated formation of the $^{C81/C96}$RIDC1$_4$ tetramer is independent of Zn(II) coordination, we prepared a second control variant, $^{A74/C81/C96}$RIDC1, which featured an alanine substituted for one of the Zn-coordinating residues, Asp74. The elimination of the Zn-Asp74 linkage was chosen because this bond is critical in the stabilization of the *i3* interface in the parent tetramer Zn$_4$:MBPC1$_4$. The yield of tetramer formation for $^{A74/C81/C96}$RIDC1 was not only unaffected in the presence or absence of Zn(II), but it was consistently higher than that of $^{C81/C96}$RIDC1 under all conditions (Figure 2c, middle panel). In the presence of 1 mM GSH/GSSG buffer, the tetramer abundance reached 77 ± 3% after 16 h, with the remaining fraction mostly in the monomeric form. Based on these results, we can conclude that the D74A mutation must stabilize the closed tetramer (species 5), although the exact molecular details of this effect are not immediately apparent.

Our third control variant was an alternative double-Cys mutant $^{C25/C96}$RIDC1, which could form the complementary *i1* interactions but had a Cys installed in position 25, which is not compatible for self-pairing in the closed tetramer (Figure 1b). In the absence of any structural bias, two Cys residues on a given protein monomer should give rise to multiple modes of disulfide-cross-linking and, in turn, the formation of open oligo- and -polymers, with no particular enrichment of any intermediate *n*-mer. This was indeed our observation with $^{C25/C96}$RIDC1 under all conditions tested (±Zn(II), ±GSH/GSSG), which formed a "ladder" of species with no distinct population of an intermediate (Figure 2c, right panel). Taken together, our observations clearly show that the hydrophobic interactions engineered into *i1* are necessary and sufficient for directing the formation of the four desired disulfide bonds.

Structural and Chemical Characterization of $^{C81/C96}$RIDC1$_4$ and Its Variants. The $^{C81/C96}$RIDC1$_4$ tetramer was purified in high yield by size-exclusion chromatography for further characterization (Figure S4 of the SI). Sedimentation velocity experiments with $^{C81/C96}$RIDC1$_4$ revealed a single, narrow peak with a maximum at 4.5 S, which slightly moved (to 4.6 S) upon addition of 4 equiv of Zn^{II}, indicating the formation of a discrete, closed tetramer that does not undergo a large conformational change upon metal binding (Figure 4a). This was confirmed through the crystal structures of apo- and Zn-bound $^{C81/C96}$RIDC1$_4$, which we determined at 2.1 and 1.2 Å resolution, respectively (Figure 4c and d; Table S1 and movies of the SI). An inspection of the core architectures of both structures (Figure 4e) reveals their striking topological resemblance to cryptands,[52] in particular spheroidal cryptands,[53] which are highly preorganized, covalently linked macropolycylic compounds designed to stably capture cations and anions in their cavities. The tetramers feature a macrocyclic base structure that is formed by the linkage of Helices 4 from each monomer by the two pairs of C96−C96′ and C81−C81′ disulfide bonds. This covalently linked macrocycle is capped from the top and the bottom by Helices 3 from each monomer, which are linked through the hydrophobic *i1* interactions and help form a central cavity lined by the four Zn coordination sites (Figure 4f). Like cryptands, this large cavity (740 Å^3 in apo-$^{C81/C96}$RIDC1$_4$, 1220 Å^3 in Zn$_4$:$^{C81/C96}$RIDC1$_4$, Figure S5

dx.doi.org/10.1021/ja405318d | J. Am. Chem. Soc. 2013, 135, 12013−12022

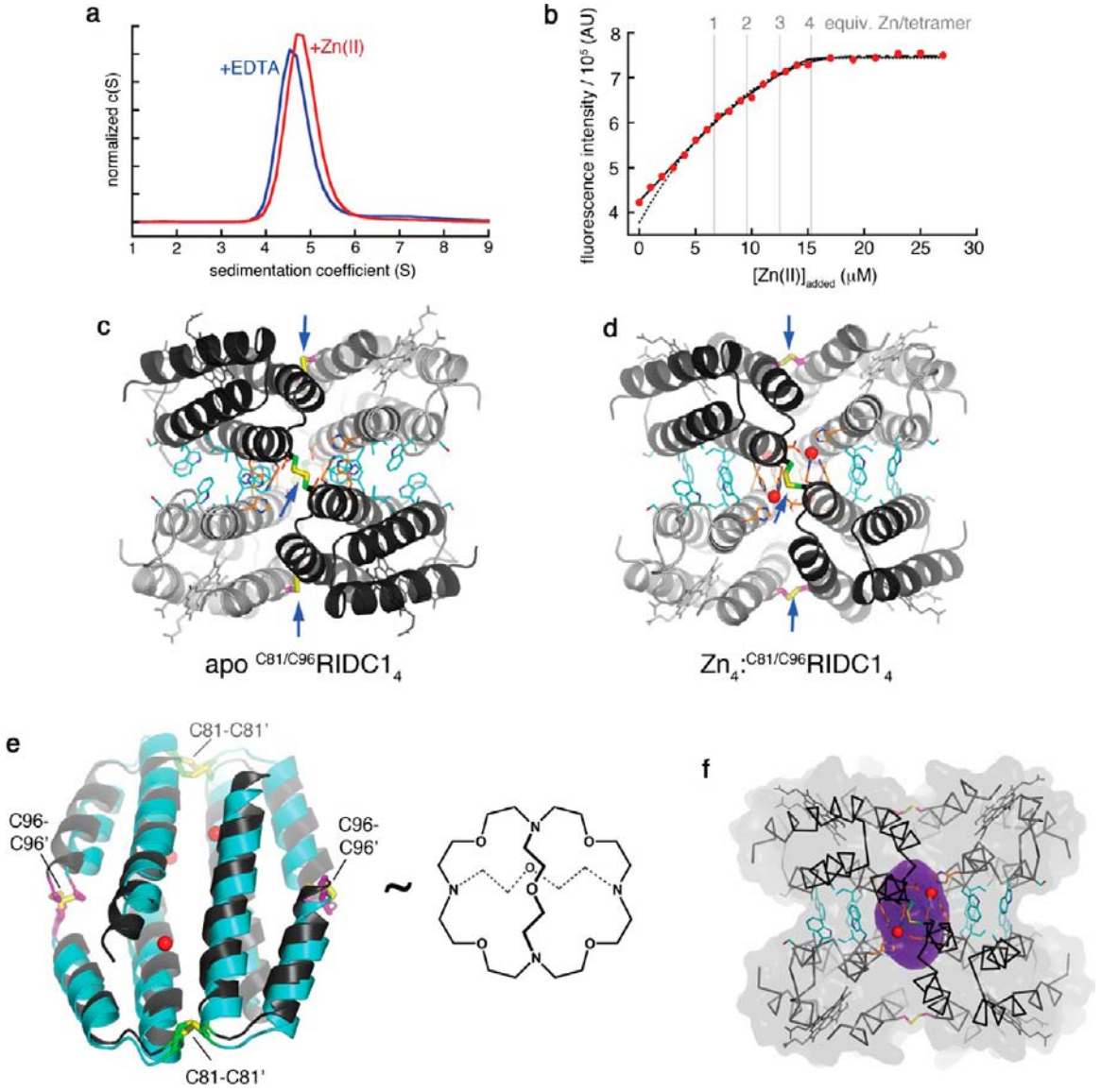

Figure 4. Structural and physicochemical characterization of apo- and Zn-bound $^{C81/C96}$RIDC1$_4$. (a) Sedimentation velocity profile of $^{C81/C96}$RIDC1$_4$ (5 μM) in the presence and absence of equimolar Zn(II). (b) Zn-binding isotherm of $^{C81/C96}$RIDC1$_4$ (2.75 μM) determined using Fura-2 (4.2 μM) as a competing ligand. Nearly equally good fits are obtained using a four consecutive Zn binding equilibrium model (1 + 1 + 1 + 1, dashed line) or a two consecutive binding equilibrium model (2 + 2, solid line), whereas a single binding equilibrium model (4 × 1, dotted line) does not appear to be adequate. (c, d) Crystal structures of apo- and Zn-bound $^{C81/C96}$RIDC1$_4$. The C81−81 and C96−C96 disulfide bonds are shown as green/yellow and magenta/yellow sticks, respectively (for close-up views of the disulfide bonds and corresponding omit electron density maps, see Figure S13 of the SI). The hydrophobic residues in the *i1* interface are highlighted in cyan. Interfacial disulfide bonds, except one C81−C81 bond in the background, are indicated with blue arrows. (e) Backbone superposition of the cryptand-like cores of apo- (cyan) and Zn-bound (dark gray) $^{C81/C96}$RIDC1$_4$ and their comparison to a synthetic spheroidal cryptand (ref 53). The cryptand-like core is composed of residues 60−96 of each of the four protein monomers. The helical segments 81−96 form the outer, covalently linked periphery, whereas the helical segments 60−81 form part of the hydrophobic *i1* interface that cap the core cavity from top and bottom (see movies of the SI). (f) The central cavity in Zn$_4$:$^{C81/C96}$RIDC1$_4$ lined by the four Zn coordination sites is highlighted in magenta.

of the SI) and the Zn coordination sites are relatively well isolated from the bulk, owing to the packing of side chains in *i1* and *i2* interfaces (movies of the SI), particularly in the case of the apo structure. Again, in analogy to cryptands, $^{C81/C96}$RIDC1$_4$ is highly preorganized for Zn(II) coordination. Structures of apo-$^{C81/C96}$RIDC1$_4$ and Zn$_4$:$^{C81/C96}$RIDC1$_4$ display a small deviation from each other, with a root-mean-square deviation (rmsd) of 2.2 Å measured over the backbone α-carbons of the cryptand-like core (Figure 4e). The small rearrangement of the metal allows Trp41 and Trp66 side chains to extend fully into the interface and preserve their original hydrophobic contacts. The Zn(II) affinity of $^{C81/C96}$RIDC1$_4$ was determined by a competition titration using the fluorescent metal indicator Fura-2 (Figure S6 of the SI), whose Zn(II) complex has a dissociation constant ($K_{d,Zn\text{-}Fura}$) of 5.7 nM.[49] These titrations revealed that $^{C81/C96}$RIDC1$_4$ bound four Zn(II) ions as expected, and the isotherm was well fit by a 2 + 2 Zn equilibrium model (i.e., two pairs of independent sites), with $K_{d1,2Zn}$= 2.6 ± 0.3 nM and $K_{d2,2Zn}$= 25 ± 4 nM (Figure 4b). ICP-OES experiments were carried out in parallel to examine the ability of $^{C81/C96}$RIDC1$_4$ to bind various divalent metal ions. These experiments showed that $^{C81/C96}$RIDC1$_4$ could indeed

dx.doi.org/10.1021/ja405318d | J. Am. Chem. Soc. 2013, 135, 12013−12022

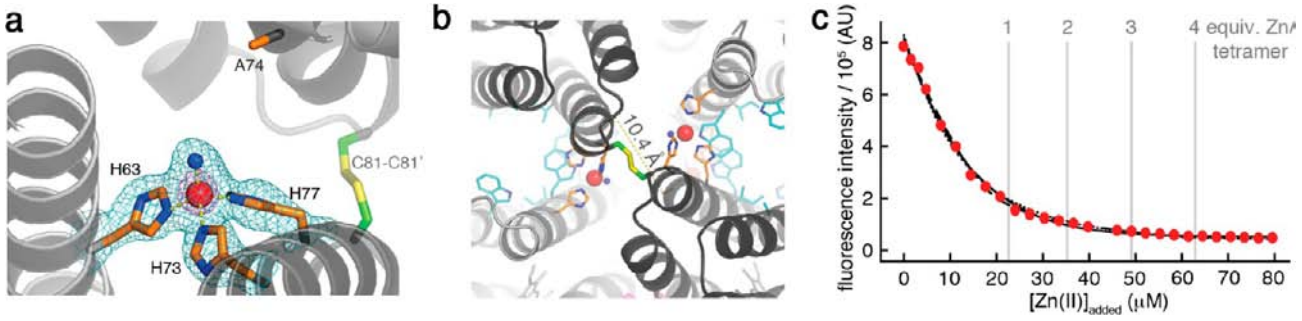

Figure 5. Structural and Zn-binding properties of $^{A74/C81/C96}$RIDC1$_4$. (a) Close-up view of one of the four identical 3His-Zn coordination sites, along with the corresponding $2F_o - F_c$ electron density map contoured at 1.4σ (cyan) and 7σ (magenta). The Zn-coordinated water molecule is shown as a blue sphere. For close-up views of the disulfide bonds and corresponding omit electron density maps, see Figure S13 of the SI. (b) View of Zn$_4$:$^{A74/C81/C96}$RIDC1$_4$ down the C_2'' axis and the *i*3 interface. The C_β–C_β distance (10.4 Å) between position 74 residues across the *i*3 interface is highlighted with a dashed line. The corresponding distance in Zn$_4$:$^{C81/C96}$RIDC1$_4$ is 8.8 Å. (c) Zn-binding isotherm of $^{A74/C81/C96}$RIDC1$_4$ (13.5 μM) determined using Mag-Fura-2 (8.7 μM) as a competing ligand. Nearly equally good fits are obtained using a four consecutive Zn binding equilibrium model (1 + 1 + 1 + 1, dashed line), a two consecutive binding equilibrium model (2 + 2, solid line), and a single binding equilibrium model (4 × 1, dotted line).

accommodate 4 Zn^{II} equivalents as well as ≤1 Co^{II}, 2 Ni^{II}, and >4 Cu^{II} ions (Figure S7 of the SI).

The fact that the self-assembly of our cryptand-like scaffold was entirely uncoupled from Zn(II) coordination suggested that it could be utilized to construct unsaturated metal coordination sites. To examine this possibility, we crystallized the Zn complex of the aforementioned $^{A74/C81/C96}$RIDC1 variant, which has the Zn-coordinating Asp74 carboxylate eliminated and can be isolated in its tetrameric form in high yield. The 2.3-Å structure of the tetramer shows that the four Zn ions are indeed coordinated only by the three original His side chains (His63, H73, and His77) and the fourth coordination site is occupied by a water molecule, closely mimicking the Zn coordination environment of carbonic anhydrases[54] and matrix metalloproteinases[55] (Figure 5). The covalently cross-linked cryptand-like topology is key to the construction of coordinatively unsaturated Zn sites, as the D74A mutant of RIDC1 (lacking C81/C96) was previously shown to form an asymmetric trimer upon Zn coordination, whereby the interfacial Zn ions were coordinatively saturated.[56] Preliminary experiments with Zn$_4$:$^{A74/C81/C96}$RIDC1$_4$ using *p*-nitrophenyl acetate (PNPA) as a substrate for potential esterase activity suggested that the buried Zn sites were not accessible to this substrate; studies are currently ongoing to "carve out" access channels to the cryptand interior.

Competition titrations using Mag-Fura-2 ($K_{d,Zn\text{-}MagFura2}$ = 47 nM)[57] (Figure 5c and Figure S8 of the SI) could be adequately described by a 4 × 1 Zn equilibrium model (i.e., four independent, equivalent binding sites), yielding $K_{d,4Zn}$ = 480 ± 35 nM for $^{A74/C81/C96}$RIDC1$_4$. This dissociation constant is approximately 1 to 2 orders of magnitude higher than those determined for $^{C81/C96}$RIDC1$_4$, consistent with the loss of a coordinating ligand. The elimination of the D74-Zn coordination leads to a slight widening of the *i*3 and subsequently the *i*1 interfaces (Figure 5b), all of which are reflected in an increased cavity volume of 2100 Å^3 (Figure S5 of the SI). Despite this potentially drastic perturbation to the inner Zn-coordination sphere, the cryptand-core of Zn$_4$:$^{A74/C81/C96}$RIDC1$_4$ is superposable onto that of Zn$_4$:$^{C81/C96}$RIDC1$_4$ with an rmsd of 1.6 Å (Figure S9 of the SI), further highlighting the structural rigidity afforded by the covalently interconnected topology.

Cellular Self-Assembly of $^{C81/C96}$RIDC1$_4$. The gene encoding for $^{C81/C96}$RIDC1 is equipped with an engineered N-terminal signal sequence, which enables the translocation of the protein upon translation into the *E. coli* periplasm, where it is processed for the covalent (*c*-type) linking of the heme cofactor to the protein backbone.[45,58] The periplasmic space is an oxidizing environment and contains the biological machinery for disulfide bond formation and exchange.[40] This raised the possibility that $^{C81/C96}$RIDC1 might correctly self-assemble into the cryptand-like tetramer in bacterial cells and, given its relatively high Zn-affinity, compete for Zn ions. To test this possibility, we performed a periplasmic extraction of the $^{C81/C96}$RIDC1-overexpressing *E. coli* cells through osmotic shock, which lyses the outer but not the inner membrane, such that any disulfide-linked products remain isolated from the cytosolic reductants. Solutions used for lysis or any other step thereafter also contained 50 mM iodoacetic acid for alkylating any free cysteines and disabling any postlysis disulfide bond formation. Crude periplasmic lysates of $^{C81/C96}$RIDC1-overexpressing cells were immediately analyzed by nonreducing, SDS-PAGE, using 3,3′,5,5′-tetramethylbenzidine (TMBZ) as the staining agent to detect heme-containing proteins[59] (Figure 6a) or Coomassie Blue to image the entire protein content (Figure S10 of the SI). The TMBZ-stained gels indicated a prominent band (~63% abundance among all stained species, Figure 6a, left panel) near the 46-kDa molecular weight marker that would correspond to the $^{C81/C96}$RIDC1$_4$ tetramer (expected mass = 49,108 Da). When SDS-PAGE was carried out after the treatment of the extracts with DTT to reduce disulfide bonds, the main band moved to where a monomeric species would be expected (Figure 6a, right panel), establishing that $^{C81/C96}$RIDC1 primarily exists as a disulfide-linked tetramer in the periplasm. A similar SDS-PAGE profile was obtained in the case of the cells that overexpressed $^{A74/C81/C96}$RIDC1 (Figure 6a), with a tetramer abundance of ~60%. In contrast, periplasmic extracts of MBPC1 and RIDC1, which do not self-assemble into tetramers in vitro, consisted almost entirely of monomers. Extracts of $^{C81/C96}$MBPC1 contained a distribution of *n*-mers with no appreciable population of a tetrameric species (Figure 6a), paralleling the findings of the self-assembly experiments carried out in vitro (Figure 1c) and reaffirming the necessity/sufficiency of hydrophobic *i*1 interactions in templating the formation of $^{C81/C96}$RIDC1$_4$. It remains to be determined whether disulfide-exchange enzymes such as

dx.doi.org/10.1021/ja405318d | J. Am. Chem. Soc. 2013, 135, 12013−12022

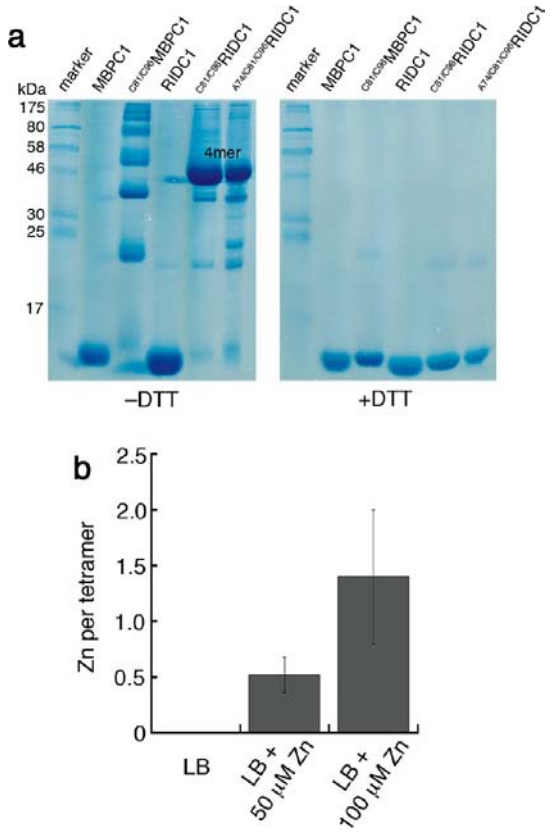

Figure 6. Disulfide-mediated self-assembly and Zn binding properties of $^{C81/C96}$RIDC1 in *E. coli* cells. (a) SDS-PAGE analysis of the periplasmic extracts of MBPC1 (lane 2), $^{C81/C96}$MBPC1 (lane 3), RIDC1 (lane 4), $^{C81/C96}$RIDC1 (lane 5), and $^{A74/C81/C96}$RIDC1 (lane 6). Electrophoresis was carried out under nonreducing conditions using untreated extracts (left panel) or DTT-treated extracts (right panel). The gels were stained with TMBZ for heme detection. For the corresponding Coomassie-stained gels, see Figure S9 of the SI. (b) ICP-OES analysis of the Zn content of self-assembled $^{C81/C96}$RIDC1$_4$ tetramers isolated from the periplasmic extracts of *E. coli* cells grown in LB media under various conditions.

DsbA ($E' \approx -100$ mV)[60] are directly involved in the self-assembly of $^{C81/C96}$RIDC1$_4$ in the periplasm.

The red-colored periplasmic extract displayed a UV–vis spectrum that was typical of reduced cyt cb_{562}, with *Q*-band maxima at 525 and 556 nm,[45] respectively (Figure S11 of the SI). The species corresponding to $^{C81/C96}$RIDC1$_4$ was isolated by size exclusion chromatography. The MALDI mass spectrum displayed a single peak at 49,133 Da in the MALDI mass spectrum (Figure S12 of the SI), slightly (25 amu) above the expected mass of the $^{C81/C96}$RIDC1$_4$ tetramer. These results establish that $^{C81/C96}$RIDC1$_4$ correctly self-assembles in *E. coli* cells; we estimate the periplasmic concentration of $^{C81/C96}$RIDC1$_4$ to be 10–20 μM (SI).

We next tested the ability of $^{C81/C96}$RIDC1$_4$ to compete for Zn(II) ions in bacterial cells. In terms of metal homeostasis, the periplasmic space of Gram-negative bacteria serves as a buffer zone that screens the cytoplasm from large environmental fluctuations in metal ion concentrations as part of the so-called envelope stress response.[61] Though not to the extent seen in the cytoplasm, competition for Zn(II) in the periplasm is still keen. The periplasmic free Zn(II) concentration is tightly regulated by transport systems such as ZnuABC ($K_{d,\ Zn\text{-}ZnuA}$ <20 nM)[62] and ZIP proteins,[63] and the periplasm contains many essential Zn-containing proteins (~20 known), including β-lactamase and superoxide dismutase.[64] In a typical experiment, $^{C81/C96}$RIDC1-expressing *E. coli* cells were grown in Luria–Bertani (LB) broth, the periplasmic $^{C81/C96}$RIDC1$_4$ tetramers were isolated using strictly metal-free buffer solutions and glassware, and their zinc and iron contents were determined via ICP-OES. Here, the iron content served as a convenient indicator of protein concentration, as each $^{C81/C96}$RIDC1 monomer contains one iron atom in the covalently bound heme cofactor. When the cells were grown in unsupplemented LB medium ($[Zn]_{LB} \approx 10$ μM),[65,66] the isolated $^{C81/C96}$RIDC1$_4$ tetramers contained no detectable amount of zinc (Figure 6b). The detection limit in these experiments was <0.1 ppm metal (lowest data point in our calibration line), which corresponded to <0.15 equiv of metal ion per tetramer. However, when the medium was supplemented with 50 or 100 μM $ZnCl_2$, the tetramers accumulated 0.52 ± 0.16 or 1.4 ± 0.6 Zn equiv, respectively (Figure 6b). No detectable amounts of other relevant divalent metal ions (Co^{II}, Ni^{II}, Cu^{II}) were found to be associated with the tetramer, and the possibility of extrinsic (nonheme) Fe^{II} binding was ruled out, as the concentration of Fe^{II} associated with the sample matched the monomeric protein concentration determined by using the extinction coefficient of the heme Soret band. Under the same experimental conditions, periplasmic extracts of non-self-assembling variants MBPC1 and RIDC1 did not contain any detectable Zn, indicating that Zn sequestration in the cell necessitates the formation of the cryptand-like tetramer. Competition by natural Zn-proteins and active regulation of the periplasmic Zn concentration likely prevent the entire population of $^{C81/C96}$RIDC1$_4$ tetramers from attaining stoichiometric Zn(II) binding. A more definitive picture would require knowledge of the concentrations and Zn-affinities of each Zn-binding protein in the periplasm alongside $^{C81/C96}$RIDC1$_4$. Nevertheless, our results indicate that $^{C81/C96}$RIDC1$_4$ is able to successfully vie for Zn(II) in cells and sequester it from the environment.

CONCLUSIONS

Despite their ubiquity in natural protein assemblies and the structural and functional advantages they confer, disulfide bonds are rarely utilized in multiples for the design and self-assembly of discrete protein architectures. Here, we have described a protein design strategy inspired by supramolecular chemistry, in which noncovalently interacting protein surfaces template the selective formation of multiple disulfide bonds across different interfaces to yield a novel, cryptand-like protein assembly in a one-pot reaction. The design of $^{C81/C96}$RIDC1 was based on the D_2 symmetry of the Zn-templated parent architecture (Zn_4:MBPC1$_4$), which presented three sets of interconnected interfaces with C_2 symmetry that guided the correct placement of Cys residues. It is important to note that D_2-symmetric tetramers are significantly overrepresented among all known tetrameric protein structures, in which the connectivity of the interfaces leads to more compact/stable structures and allows facile incorporation of function or allostery.[67,68]

The structure and design of $^{C81/C96}$RIDC1$_4$ is noteworthy from several viewpoints. Owing to its cryptand-like topology and connectivity, $^{C81/C96}$RIDC1$_4$ is highly preorganized for metal binding in its interior and possesses a large, protected cavity in its center. Both of these structural features are

prominent characteristics of natural metalloenzyme architectures but challenging goals for *de novo* protein design.[69,70] In fact, the most successful metalloprotein/enzyme design approaches largely bypass the protein folding problem by utilizing either existing protein folds[71−73] or canonical folding motifs (e.g., α-helical coiled coils)[74,75] whose interiors are engineered/repurposed for constructing metal binding sites. Second, $^{C81/C96}$RIDC1$_4$ illustrates an important advantage of using noncovalently (or "remotely") templated disulfide bonds for engineering tailorable protein architectures. Namely, the three pairs of interfaces that make up $^{C81/C96}$RIDC1$_4$ (*i1*, *i2*, and *i3*) bury a total surface area of nearly ∼5000 Å^2 excluding the interior cavity, yet the total surface area of designed noncovalent interactions in *i1* (which are sufficient for directing disulfide bond formation across *i2* and *i3*) cover only 2000 Å^2. This suggests that a significant portion of the *i2* and *i3* interfaces, which are solely connected through disulfide bonds, may be subjected to alterations—for example, to carve out access channels to the interior cavity—without disrupting the overall structure of the assembly. Hypothetically, engineering a stable architecture similar to $^{C81/C96}$RIDC1$_4$ purely through noncovalent interactions would not only require the design of all three interfaces (i.e., covering close to 5000 Å^2), but the resulting architecture would also be far more sensitive to alterations in its interfaces. Third, $^{C81/C96}$RIDC1 (a protein that self-assembles into a metalloenzyme-like supramolecular architecture) is separated from its progenitor cyt cb_{562} (a putative electron transfer protein) by only 11 surface point mutations; that is, they share ∼90% sequence identity. This feature recapitulates, in a synthetic system, how nature can take advantage of a limited number of protein domains and folding motifs to create entirely new structures and functions.[76] Finally, $^{C81/C96}$RIDC1$_4$ is a synthetic supramolecular complex, yet it consists of entirely natural components and is able to correctly self-assemble in bacterial cells and incorporate the desired metal ion in a highly competitive environment. This raises the tantalizing prospect of constructing novel supramolecular or bioinorganic scaffolds in living systems that can be subjected to selective pressure for the evolution of new and improved biological functions.

MATERIALS AND METHODS

Disulfide-Mediated $^{C81/C96}$RIDC1 Self-Assembly. Upon purification (see SI), $^{C81/C96}$RIDC1 was concentrated to 2−4 mM in an Amicon stirred cell using a 10-kDa cutoff membrane. To the $^{C81/C96}$RIDC1 stock solution was added an excess (100 mM) of dithiothreitol (DTT) to dissociate any disulfide bonds. After a 30-min incubation, the protein solution was eluted through a 10DG desalting column (BioRad) to remove DTT, using a running buffer solution of 50 mM TRIS (pH 7) and 150 mM NaCl. The protein concentration was adjusted to 50 μM using the same buffer solution. Immediately, several 20-μL aliquots of the protein solution were transferred to 0.65-mL centrifuge tubes, and to these aliquots were added either 1 mol equiv of $ZnCl_2$, 1 mM 1:19 GSH/GSSG, 1 mM 19:1 GSH/GSSG, or nothing. Samples were incubated under air exposure, either at room temperature or in an Eppendorf thermocycler at 35 °C. Aliquots (1-μL) from each sample were taken at desired time intervals over a period of 24 h; any remaining free cysteines in these solutions were passivated by addition of 50 mM iodoacetic acid and nonreducing SDS-PAGE loading buffer (bromophenol blue, 10% SDS, glycerol, 1.5 M Tris, pH 6.8). The aliquots were applied to 12% SDS-PAGE gels and run for 40 min at 400 V in a BioRad MiniProtean TetraCell box. Gels were stained with Coomassie Blue for 10 min and then destained for 1−2 h in a 10% nitric acid/30% methanol solution. They were then imaged using a scanner, and protein band intensities were integrated using ImageJ.[77]

Preparation and Isolation of Tetrameric $^{C81/C96}$RIDC1$_4$ and $^{A74/C81/C96}$RIDC1$_4$. As described above, purified and concentrated $^{C81/C96}$RIDC1 (2−4 mM) was first treated with DTT to reduce any preformed disulfide bonds. After removal of DTT, to the protein stock solution was added 1 mM of 1:19 GSH/GSSG and the solution was incubated at 35 °C for 16−20 h to form the $^{C81/C96}$RIDC1$_4$ tetramer in high yield. The tetramer was isolated from other oligomeric species by fast protein liquid chromatography on a DuoFlow workstation (Bio-Rad), using a XK26/100 column (GE Healthcare) packed with Superdex 75 (GE Healthcare) and a running buffer solution of 20 mM TRIS (pH 7) and 150 mM NaCl (Figure S4 of the SI). The tetramer fraction was identified by SDS-PAGE under nonreducing conditions. The tetramer was concentrated, and excess EDTA (>10 mM) was added to remove any metal ions bound to the protein during purification. The protein stock solution was exchanged into a Chelex-treated buffer solution of 20 mM MOPS (pH 7) and 150 mM NaCl, flash-frozen in 200-μL aliquots and kept at −80 °C until further use.

Periplasmic Protein Extraction and Heme Staining. A 1-L cell culture expressing the protein variant of interest was harvested after 16 h of growth by centrifugation, and the cell pellet (∼7 g) was washed three times with a resuspension buffer (10 mM TRIS, pH 7.4, 33 mM NaCl). Cold osmotic shock was performed by first suspending the cell pellet in 10 volumes of the resuspension buffer (70 mL), followed by the addition of 10 volumes of 40% sucrose (70 mL) and excess iodoacetic acid (>50 mM). After incubation in an ice bath for 10 min, the cell suspension was centrifuged at 6000 rpm, and the cell pellet was resuspended with 20 volumes (140 mL) of ice-cold solution of 10 mM TRIS (pH 7.4), 0.5 mM $MgCl_2$, and 50 mM iodoacetic acid. After another 10-min incubation, the cell suspension was once again centrifuged (20 min, 8000 rpm), whereby the supernatant contained the red-colored periplasmic extract. The supernatant was concentrated using an Amicon stirred cell, and 15 μL of the concentrated sample was run on a nonreducing, 12% SDS-PAGE gel for 40 min at 400 mV. The gel was immersed in a solution of 30 mL of 6.3 mM tetramethylbenzidine (TMBZ) and 70 mL of 0.25 M sodium acetate (pH 5) in the dark for 1−2 h, after which 30 mM hydrogen peroxide was added to the solution. The gel was incubated for another 30 min to allow full development of heme-containing bands, which were imaged on a scanner and integrated using ImageJ.[77]

Competitive Zn(II) Binding Titrations. A 1-mL solution containing 4 μM Fura-2 (Life Technologies) and 2−3 μM $^{C81/C96}$RIDC$_4$ was titrated in a 1-cm cuvette with 1−2 μL aliquots of 1 mM $ZnCl_2$. After each addition, the sample was equilibrated for at least 5 min at room temperature, upon which the excitation scan was recorded on a Horiba Fluorolog 2 fluorimeter using an excitation range of 250−450 nm and detection at 510 nm. The change in excitation intensity at 335 nm was plotted versus Zn(II) concentration, and the resulting curve was fit alternatively to 1 × 4 Zn, 2 × 2 Zn, or 4 × 1 Zn binding models using Dynafit[78] as described previously.[49] A similar protocol was used in the case of $^{A74/C81/C96}$RIDC1$_4$ (13.5 μM) in competition titration experiments with Mag-Fura-2 (Life Technologies) (8.7 μM, excitation range of 300−400 nm, emission detection at 505 nm). The change in excitation intensity at 370 nm was plotted versus Zn(II) concentration, and the resulting curve was fit alternatively to 1 × 4 Zn, 2 × 2 Zn, or 4 × 1 Zn binding models by Dynafit.

ASSOCIATED CONTENT

Supporting Information

Supporting Methods, Supporting Figures S1−S13, Supporting Movies S1 and S2 and Supporting Table S1 are available. This material is available free of charge via the Internet at http://pubs.acs.org.

AUTHOR INFORMATION

Corresponding Author

tezcan@ucsd.edu

Notes

The authors declare no competing financial interest.

ACKNOWLEDGMENTS

We thank Dr. Woon Ju Song for helpful discussions and experimental guidance. Portions of this research were carried out at SSRL, operated by Stanford University on behalf of DOE. This work was supported by NSF (CHE-0908115), the Beckman Foundation, and the Sloan Foundation. F.A.T. was additionally supported by DOE-BES, Division of Materials Sciences and Engineering under the award DE-FG02-10ER46677 (protein crystallography), A.M.-M. by a traineeship under the NIH Cell and Molecular Genetics Training Grant, and A.P. by the UCSD MARC (NIH) and Amgen Scholars programs.

REFERENCES

(1) Busch, D. H. *J. Inclusion Phenom.* **1992**, *12*, 389.
(2) Anderson, S.; Anderson, H. L.; Sanders, J. K. M. *Acc. Chem. Res.* **1993**, *26*, 469.
(3) McMurry, T. J.; Raymond, K. N.; Smith, P. H. *Science* **1989**, *244*, 938.
(4) Furlan, R. L. E.; Otto, S.; Sanders, J. K. M. *Proc. Natl. Acad. Sci. U.S.A.* **2002**, *99*, 4801.
(5) Thompson, M. C.; Busch, D. H. *J. Am. Chem. Soc.* **1964**, *86*, 3651.
(6) Day, V. W.; Marks, T. J.; Wachter, W. A. *J. Am. Chem. Soc.* **1975**, *97*, 4519.
(7) Byrne, G. T.; Linstead, R. P.; Lowe, A. R. *J. Chem. Soc.* **1934**, 1017.
(8) McMurry, T. J.; Rodgers, S. J.; Raymond, K. N. *J. Am. Chem. Soc.* **1987**, *109*, 3451.
(9) Creaser, I. I.; Geue, R. J.; Harrowfield, J. M.; Herlt, A. J.; Sargeson, A. M.; Snow, M. R.; Springborg, J. *J. Am. Chem. Soc.* **1982**, *104*, 6016.
(10) Sauvage, J. P. *Acc. Chem. Res.* **1990**, *23*, 319.
(11) Cantrill, S. J.; Chichak, K. S.; Peters, A. J.; Stoddart, J. F. *Acc. Chem. Res.* **2004**, *38*, 1.
(12) Ponnuswamy, N.; Cougnon, F. B. L.; Clough, J. M.; Pantos, G. D.; Sanders, J. K. M. *Science* **2012**, *338*, 783.
(13) Beves, J. E.; Blight, B. A.; Campbell, C. J.; Leigh, D. A.; McBurney, R. T. *Angew. Chem., Int. Ed.* **2011**, *50*, 9260.
(14) Aldaye, F. A.; Sleiman, H. F. *J. Am. Chem. Soc.* **2007**, *129*, 10070.
(15) Lee, D. H.; Granja, J. R.; Martinez, J. A.; Severin, K.; Ghadiri, M. R. *Nature* **1996**, *382*, 525.
(16) Yao, S.; Ghosh, I.; Zutshi, R.; Chmielewski, J. *J. Am. Chem. Soc.* **1997**, *119*, 10559.
(17) Carnall, J. M. A.; Waudby, C. A.; Belenguer, A. M.; Stuart, M. C. A.; Peyralans, J. r. m. J.-P.; Otto, S. *Science* **2010**, *327*, 1502.
(18) Clark, T. D.; Ghadiri, M. R. *J. Am. Chem. Soc.* **1995**, *117*, 12364.
(19) Krishnan-Ghosh, Y.; Balasubramanian, S. *Angew. Chem., Int. Ed. Engl.* **2003**, *42*, 2171.
(20) Hartgerink, J. D.; Beniash, E.; Stupp, S. I. *Science* **2001**, *294*, 1684.
(21) Cougnon, F. B. L.; Sanders, J. K. M. *Acc. Chem. Res.* **2011**, *45*, 2211.
(22) Corbett, P. T.; Leclaire, J.; Vial, L.; West, K. R.; Wietor, J.-L.; Sanders, J. K. M.; Otto, S. *Chem. Rev.* **2006**, *106*, 3652.
(23) Sadownik, J. W.; Ulijn, R. V. *Curr. Opin. Biotechnol.* **2010**, *21*, 401.
(24) Sinclair, J. C.; Davies, K. M.; Venien-Bryan, C.; Noble, M. E. M. *Nat. Nanotechnol.* **2011**, *6*, 558.
(25) King, N. P.; Sheffler, W.; Sawaya, M. R.; Vollmar, B. S.; Sumida, J. P.; André, I.; Gonen, T.; Yeates, T. O.; Baker, D. *Science* **2012**, *336*, 1171.
(26) Lai, Y.-T.; Cascio, D.; Yeates, T. O. *Science* **2012**, *336*, 1129.
(27) Fletcher, J. M.; Harniman, R. L.; Barnes, F. R. H.; Boyle, A. L.; Collins, A.; Mantell, J.; Sharp, T. H.; Antognozzi, M.; Booth, P. J.; Linden, N.; Miles, M. J.; Sessions, R. B.; Verkade, P.; Woolfson, D. N. *Science* **2013**, *340*, 595.
(28) Padilla, J. E.; Colovos, C.; Yeates, T. O. *Proc. Natl. Acad. Sci. U.S.A.* **2001**, *98*, 2217.
(29) Singh, R.; Whitesides, G. M. In *Sulphur-Containing Functional Groups*; John Wiley & Sons, Inc.: 1993; p 633.
(30) Perry, L. J.; Wetzel, R. *Science* **1984**, *226*, 555.
(31) Wells, J. A.; Powers, D. B. *J. Biol. Chem.* **1986**, *261*, 6564.
(32) Sauer, R. T.; Hehir, K.; Stearman, R. S.; Weiss, M. A.; Jeitlernilsson, A.; Suchanek, E. G.; Pabo, C. O. *Biochemistry* **1986**, *25*, 5992.
(33) Gokhale, R. S.; Agarwalla, S.; Francis, V. S.; Santi, D. V.; Balaram, P. *J. Mol. Biol.* **1994**, *235*, 89.
(34) Scrutton, N. S.; Berry, A.; Perham, R. N. *FEBS Lett.* **1988**, *241*, 46.
(35) Shirakawa, M.; Matsuo, H.; Kyogoku, Y. *Protein Eng.* **1991**, *4*, 545.
(36) Banatao, D. R.; Cascio, D.; Crowley, C. S.; Fleissner, M. R.; Tienson, H. L.; Yeates, T. O. *Proc. Natl. Acad. Sci. U. S. A.* **2006**, *103*, 16230.
(37) Singh, R.; Whitesides, G. M. In *Sulphur-Containing Functional Groups*; John Wiley & Sons, Inc.: 1993, p 633 (published online 2010).
(38) Royo, M.; Contreras, M. Ä.; Giralt, E.; Albericio, F.; Pons, M. *J. Am. Chem. Soc.* **1998**, *120*, 6639.
(39) Wu, C.; Leroux, J.-C.; Gauthier, M. A. *Nat. Chem.* **2012**, *4*, 1044.
(40) Mamathambika, B. S.; Bardwell, J. C. *Ann. Rev. Cell Dev. Biol.* **2008**, *24*, 211.
(41) Craik, D. J. *Nat. Chem.* **2012**, *4*, 600.
(42) Salgado, E. N.; Radford, R. J.; Tezcan, F. A. *Acc. Chem. Res.* **2010**, *43*, 661.
(43) Radford, R. J.; Brodin, J. D.; Salgado, E. N.; Tezcan, F. A. *Coord. Chem. Rev.* **2011**, *255*, 790.
(44) Brodin, J. D.; Ambroggio, X. I.; Tang, C. Y.; Parent, K. N.; Baker, T. S.; Tezcan, F. A. *Nat. Chem.* **2012**, *4*, 375.
(45) Faraone-Mennella, J.; Tezcan, F. A.; Gray, H. B.; Winkler, J. R. *Biochemistry* **2006**, *45*, 10504.
(46) Salgado, E. N.; Faraone-Mennella, J.; Tezcan, F. A. *J. Am. Chem. Soc.* **2007**, *129*, 13374.
(47) Salgado, E. N.; Lewis, R. A.; Mossin, S.; Rheingold, A. L.; Tezcan, F. A. *Inorg. Chem.* **2009**, *48*, 2726.
(48) Salgado, E. N.; Ambroggio, X. I.; Brodin, J. D.; Lewis, R. A.; Kuhlman, B.; Tezcan, F. A. *Proc. Natl. Acad. Sci. U.S.A.* **2010**, *107*, 1827.
(49) Brodin, J. D.; Medina-Morales, A.; Ni, T.; Salgado, E. N.; Ambroggio, X. I.; Tezcan, F. A. *J. Am. Chem. Soc.* **2010**, *132*, 8610.
(50) Jones, D. P. In *Methods in Enzymology*; Helmut, S., Lester, P., Eds.; Academic Press: 2002; Vol. *348*, p 93.
(51) Cleland, W. W. *Biochemistry* **1964**, *3*, 480.
(52) Lehn, J. M. *Acc. Chem. Res.* **1978**, *11*, 49.
(53) Graf, E.; Lehn, J. M. *J. Am. Chem. Soc.* **1975**, *97*, 5022.
(54) Christianson, D. W.; Fierke, C. A. *Acc. Chem. Res.* **1996**, *29*, 331.
(55) Lovejoy, B.; Cleasby, A.; Hassell, A. M.; Longley, K.; Luther, M. A.; Weigl, D.; McGeehan, G.; McElroy, A. B.; Drewry, D.; Lambert, M. H.; Jordan, S. R. *Science* **1994**, *263*, 375.
(56) Ni, T. W.; Tezcan, F. A. *Angew. Chem., Int. Ed.* **2010**, *49*, 7014.
(57) Salgado, E. N.; Brodin, J. D.; To, M. M.; Tezcan, F. A. *Inorg. Chem.* **2011**, *50*, 6323.
(58) Braun, M.; Thony-Meyer, L. *Proc. Natl. Acad. Sci. U.S.A.* **2004**, *101*, 12830.
(59) Thomas, P. E.; Ryan, D.; Levin, W. *Anal. Biochem.* **1976**, *75*, 168.
(60) Wunderlich, M.; Glockshuber, R. *Protein Sci.* **1993**, *2*, 717.

(61) Raivio, T. L. *Mol. Microbiol.* **2005**, *56*, 1119.
(62) Yatsunyk, L. A.; Easton, J. A.; Kim, L. R.; Sugarbaker, S. A.; Bennett, B.; Breece, R. M.; Vorontsov, I. I.; Tierney, D. L.; Crowder, M. W.; Rosenzweig, A. C. *J. Biol. Inorg. Chem.* **2008**, *13*, 271.
(63) Guerinot, M. L. *Biochem. Biophys. Acta* **2000**, *1465*, 190.
(64) Hantke, K. *Curr. Opin. Microbiol.* **2005**, *8*, 196.
(65) Outten, C. E.; O'Halloran, T. V. *Science* **2001**, *292*, 2488.
(66) Taylor, P. K.; Parks, B. Y. A.; Kurtz, D. M.; Amster, I. J. *J. Biol. Inorg. Chem.* **2001**, *6*, 201.
(67) Goodsell, D. S.; Olson, A. J. *Annu. Rev. Biophys. Struct.* **2000**, *29*, 105.
(68) Janin, J. l. *Science* **2008**, *319*, 165.
(69) Lu, Y.; Yeung, N.; Sieracki, N.; Marshall, N. M. *Nature* **2009**, *460*, 855.
(70) Der, B. S.; Edwards, D. R.; Kuhlman, B. *Biochemistry* **2012**, *51*, 3933.
(71) Park, H.-S.; Nam, S.-H.; Lee, J. K.; Yoon, C. N.; Mannervik, B.; Benkovic, S. J.; Kim, H.-S. *Science* **2006**, *311*, 535.
(72) Khare, S. D.; Kipnis, Y.; Greisen, P., Jr.; Takeuchi, R.; Ashani, Y.; Goldsmith, M.; Song, Y.; Gallaher, J. L.; Silman, I.; Leader, H.; Sussman, J. L.; Stoddard, B. L.; Tawfik, D. S.; Baker, D. *Nat. Chem. Biol.* **2012**, *8*, 294.
(73) Koehler, V.; Wilson, Y. M.; Duerrenberger, M.; Ghislieri, D.; Churakova, E.; Quinto, T.; Knoerr, L.; Haussinger, D.; Hollmann, F.; Turner, N. J.; Ward, T. R. *Nat. Chem.* **2013**, *5*, 93.
(74) Reig, A. J.; Pires, M. M.; Snyder, R. A.; Wu, Y.; Jo, H.; Kulp, D. W.; Butch, S. E.; Calhoun, J. R.; Szyperski, T. G.; Solomon, E. I.; DeGrado, W. F. *Nat. Chem.* **2012**, *4*, 900.
(75) Zastrow, M. L.; Peacock, F. A.; Stuckey, J. A.; Pecoraro, V. L. *Nat. Chem.* **2012**, *4*, 118.
(76) Chothia, C.; Gough, J.; Vogel, C.; Teichmann, S. A. *Science* **2003**, *300*, 1701.
(77) Schneider, C. A.; Rasband, W. S.; Eliceiri, K. W. *Nat. Methods* **2012**, *9*, 671.
(78) Kuzmic, P. *Anal. Biochem.* **1996**, *237*, 260.